Arch. Metall. Mater. **62** (2017), 4, 2433-2440

DOI: 10.1515/amm-2017-0358

M. KRÓL*#, T. MIKUSZEWSKI**, D. KUC***, T. TAŃSKI*, E. HADASIK**

THERMAL ASSESSMENT OF MODIFIED ULTRA-LIGHT MAGNESIUM-LITHIUM ALLOYS

The paper presents the results of the influence of commercial TiBor and AlSr10 master alloys on the refine the grains size, hardness and crystallisation process based on the thermal-derivation analysis of light cast magnesium-lithium-aluminium alloys. The effects of TiBor and AlSr10 content on the characteristic parameters of the crystallisation process of Mg-Li-Al alloys were investigated by thermal-derivative analysis (TDA). Microstructural evaluations were identified by light microscope, X-ray diffraction, scanning electron microscopy, and energy dispersive X-ray spectroscopy.

The results showed that the addition of TiBor master alloy reduced the grain size of Mg-9Li-1.5Al cast alloy from 900 μm to 500 μm, while the addition of AlSr10 master alloy reduced the grain size of investigated cast alloy from 900 μm to 480 μm. Moreover, an addition of TiBor and AlSr10 simultaneously reduced the grain size from 900 μm to 430 μm.

Results from the thermal-derivative analysis showed that the addition of grain refinement causes a decrease in nucleation temperature and solidus temperature.

Keywords: cast magnesium-lithium alloys, crystallisation, thermal-derivative analysis, grain refinement

1. Introduction

There is considerable interest in the development of the magnesium alloys since it is the lightest amongst all non-ferrous metals. Magnesium is the lightest metal that can be applied in structural applications when combined with other elements [1,2]. Magnesium alloys have newly been adopted to make portable electric devices because these alloys are light, exhibit high electrical and thermal conductivities, and can be recycled [3]. They have also been used in automotive and aerospace applications due to their attractive attributes containing low density, high specific strength and a superior stiffness-to-weight ratio comparing to the other construction materials [4-7].

The magnesium-lithium alloys with Li contents ranging from 4 to 12 mass% show a dual-phase composition of Mg-rich (α-hcp) and Li-rich (β-bcc) phases. This dual-phase composition has great formability and extra-low density but manifests a reduced mechanical property and a weak corrosion resistance [2,8-10].

The addition of lithium to magnesium alloys complicates the technological process of melting and casting of these alloys. It's difficult to prepare a batch for the melting, because the lithium reacts with the oxygen and water from the atmosphere, and with nitrogen, and is reacted with CO_2 to the form of lithium carbonate. A liquid solution of magnesium with lithium is more aggressive than the liquid magnesium in contact with the ceramic crucible materials, covers of the thermocouples, and the ceramic moulding material. Due to its low melting point and ease of evaporation becomes necessary careful control of temperature melting magnesium alloys with lithium, to prevent overheating of the liquid alloy [11-13].

These microstructures are very attractive from mechanical properties, and it is of both scientific and technological interest to investigate whether such structures may be effected in Mg-Al alloys to which Li is added to reduce the density. Therefore, the microstructures of solidified Mg-Li-Al alloys modified by TiBor and Sr have been studied [9,14-16].

Magnesium alloys contain an insufficient number of active nucleating particles to initiate solidification. A high degree of undercooling is required to initiate crystallisation in unrefined Mg alloys due to the poor nucleating strength of these particles. An easier way to obtain useful nucleating particles is through the addition of grain refiners. Grain refiners are commonly used in the industry to improve the mechanical properties and castability of alloys.

The use of titanium Ti-B based refiners, such as the commercially available TiBor, is very popular in Mg alloys but not so much in Mg-Li alloys. Grain refinement occurs with Ti-B based refiners due to the formation of the TiB_2 particle. Recently, there

* SILESIAN UNIVERSITY OF TECHNOLOGY, FACULTY OF MECHANICAL ENGINEERING, INSTITUTE OF ENGINEERING MATERIALS AND BIOMATERIALS, 18A KONARSKIEGO STR., 44-100 GLIWICE, POLAND

** SILESIAN UNIVERSITY OF TECHNOLOGY, FACULTY OF MATERIALS ENGINEERING AND METALLURGY, INSTITUTE OF METALS TECHNOLOGY, 8 KRASIŃSKIEGO STR., 40-019 KATOWICE, POLAND

*** SILESIAN UNIVERSITY OF TECHNOLOGY, FACULTY OF MATERIALS ENGINEERING AND METALLURGY, INSTITUTE OF MATERIALS SCIENCE , 8 KRASIŃSKIEGO ST., 40-019 KATOWICE, POLAND

Corresponding author: mariusz.krol@polsl.pl

has been research on the viability of adding master alloys that form TiB_2 particles within Mg melts. These popular master alloys are often Al-Ti-B based [2]. For instance, Wang et al. [9] used a TiBor master alloy at 0.3 wt.% to successfully refine the grains in the AZ31B alloy. The reduction in grain size was significant, with a decrease of approximately 90% [3].

The application of strontium (Sr) as a grain refiner has been studied, and one theory has been proposed. As stated by Cheng et al. [15], concluded that Sr caused grain refinement because of the low solubility (0.11%) of Sr in Mg. This low solubility allowed for Sr to enrich the liquid ahead of the solid interface, causing constitutional undercooling (or grain growth restriction). It must be noticed that the modification by Sr is effective only for pure magnesium or low aluminium content magnesium alloys [3,9,11].

No research has been found with the focus on studying the effect of grain refiner addition on crystallisation process of Mg-Li-Al alloys. Based on the above, it appears that by combining the effects of TiBor and Sr and utilising the benefits of TDA, an optimum combination of properties may be achieved.

The alloys studied have been chosen by past work on the thermal analysis of Mg metal alloys, where it has been established that a thermal-derivative analysis can be a powerful and useful tool to sufficiently describe a solidification pathway of magnesium alloys [1,17-20].

To understand the effect of grain refinements as TiBor and Sr on Mg-Li-Al alloys, it is important to understand the phase stability of the as cast Mg-Li-Al alloys. The study also focusses on the evolution of the microstructure of light Mg-Li alloys and their mechanical properties.

2. Experimental procedure

Within the framework of present work alloys of magnesium with lithium and aluminium and with grain refinements such as TiBor and AlSr10 have been melt, cast and investigate.

As main components used in experiments, magnesium with technical grade (min. 99.5% Mg), aluminium 3N8 (99.98% Al), lithium (99.9% Li), and refinements in the form of cement containing titanium and boron (AlTi5B) and strontium (AlSr10) were utilised. Melting and casting of alloys were carried out using laboratory vacuum induction furnace VSG 02 from the company Balzers. Melts carried out in a crucible of Al_2O_3 in shape of ø60×80 mm, using the ceramic material sheath thermocouple for measuring the temperature of melting and casting alloys.

Magnesium, lithium and aluminium were placed directly in the crucible. Before melting, after closing the furnace, repeatedly pumped out a working chamber of the furnace, blowing with argon. As a result, it minimises the residual amount of oxygen in the chamber, which could cause contamination and oxidation of the prepared alloy. Melts were carried out in argon at a pressure of 650 Tr, to minimise the evaporation starting components. Melting temperature was approx. 700÷720°C and the melting time approx. 5 min., which, taking into account the strong bath stirring electrodynamic eddy currents in enough for the complete homogenization of the melt. Grain refinements were introduced at the end of the melting process from the vacuum containers. After placed of grain refinements in the alloy, melts kept in the liquid state for 2 minutes, followed by the casting.

Alloys were cast by gravity into the cold mould of graphite to give rod-shaped ingots with dimensions ø20×100 mm. Ingots were characterised by a homogeneous, fine-grained structure and not found to the occurrence of casting defects.

The chemical composition of the as-received TiBor and AlSr10 master alloys used for Ti and Sr additions is given in Table 1.The chemical composition of achieved alloys is presented in Table 2.

TABLE 1

Chemical composition of commercial master alloys used as modifiers

TiBor					AlSr10			
Ti [%]	B [%]	Fe [%]	Si [%]	V [%]	Sr [%]	Fe [%]	Si [%]	Ca [%]
4.9	0.95	0.17	0.06	0.09	10.07	0.13	0.08	<0.10

TABLE 2

Chemical composition of formed Mg-Li-Al alloys

Elements, [% wt.]				
Li	Al	AlTi5B	AlSr10	Mg
9.0	1.5	—	—	Balance
9.0	1.5	0.2	—	Balance
9.0	1.5	—	0.2	Balance
9.0	1.5	0.2	0.2	Balance

The densities of developed ultra-light Mg-Li alloys have been measured by using the Archimedes principle. Analytical balance Adventurer Pro realised measurements with special density determination kit. To limit measure error, measurements were repeated six times. To measure a density of developed Mg-Li-Al alloys, distilled water with the density of 1 g/cm3 was used.

The thermal-derivative analysis was done on the prepared cylindrical samples in shape of 18 mm in diameter and 20 mm. Samples were melted at 700°C in an argon atmosphere. After isothermal holding for 90 s, all the melts were solidified and cooled to room temperature in the crucibles with argon protection in the furnace to minimise the oxidation. Metallographic specimens were horizontally sliced at the position that is 10 mm from the bottom. The as-cast grains of the etched samples were examined using polarised light in optical microscope Leica equipped Q-WinTM image analyser. The grain size was measured by the linear intercept method at the centre of transverse sections.

The X-ray qualitative and quantitative microanalysis and the analysis of a surface concentration of cast elements in the examined magnesium-lithium cast alloy have been made on the scanning electron microscope ZEISS SUPRA 35 with a system EDAX XM4 TRIDENT consisting of spectrometer EDS, WDS and EBSD.

Phase composition was determined by the X-ray diffraction technique utilising the X`Pert apparatus including a cobalt

lamp with 40 kV voltage. The calculation was performed by angle range of 2Q: 30°-110°. The measurement step was 0.03° in length while the pulse counting time was the 30s.

3. Results and discussion

Density measurements show that all of the grain refinement of magnesium alloys reveal density about 1.5 g/cm^3.

The optical micrograph of the as cast Mg-Li-Al alloys without and with the additions of TiBor and Sr master alloys are shown in Figure 1. The investigated alloys consist of two major phase fields, which are hcp α-(Mg) phase (elongated ribbon-like) and bcc β-Li matrix (a dark area between α-(Mg) phase) which is in consistent with the Mg-Li binary system [20-22]. Based on the computer image analysis was found that fraction of α-(Mg) phase to β-(Li) phase is 38 to 62%. It can be concluded that analysed Mg-Li-Al alloys have hyper-eutectic structure. The identity of the phases in the optical micrographs is established on the basis that the β-(Li) major phase in Fig. 1 is slightly shaded. Based on analysis of Fig. 1b,d it can be seen that granular particle-like are randomly depressively distributed in the α and β matrix. EDS results of analysed intermetallic compounds revealed a high concentration of Al, Sr and Mg though Mg may come from the matrix. The observed intermetallic compounds have most probably resulted from the grain refinements addition in the form of $Mg_{17}Sr_2$, Mg_2Sr or Al_4Sr phase as suggested in [23-25], however, it must be noted that melting temperatures of proposed phases are 606°C, 680°C and 1040°C, respectively. Moreover, according to the Mg-Sr binary system [22] and suggestions in [23], the Mg_2Sr phase is observed Mg alloys with a higher concentration of Sr (more than 1.5%). With the TiBor and AlSr10 addition, notable grain refinement occurs in alloys. Furthermore, optical metallography showed sufficiently dense metals.

The qualitative X-ray microanalysis confirmed chemical composition of analysed phases, and it is presented in Figs. 2-4. SEM image of the as-cast Mg-9Li-1.5Al alloy with the addition of TiBor (Fig. 2) show that granular particle with irregular shape exists in the α-(Mg) phase. An EDS is performed at the specific location which is pointed as 3 in the compound area, which reveals that these compounds consist of a high concentration of Mg and Al elements. It must be noted, that due to limitations of a scanning microscope, in all investigated Mg-Li-Al alloys presence of Li was not observed during the measurements (e.g.

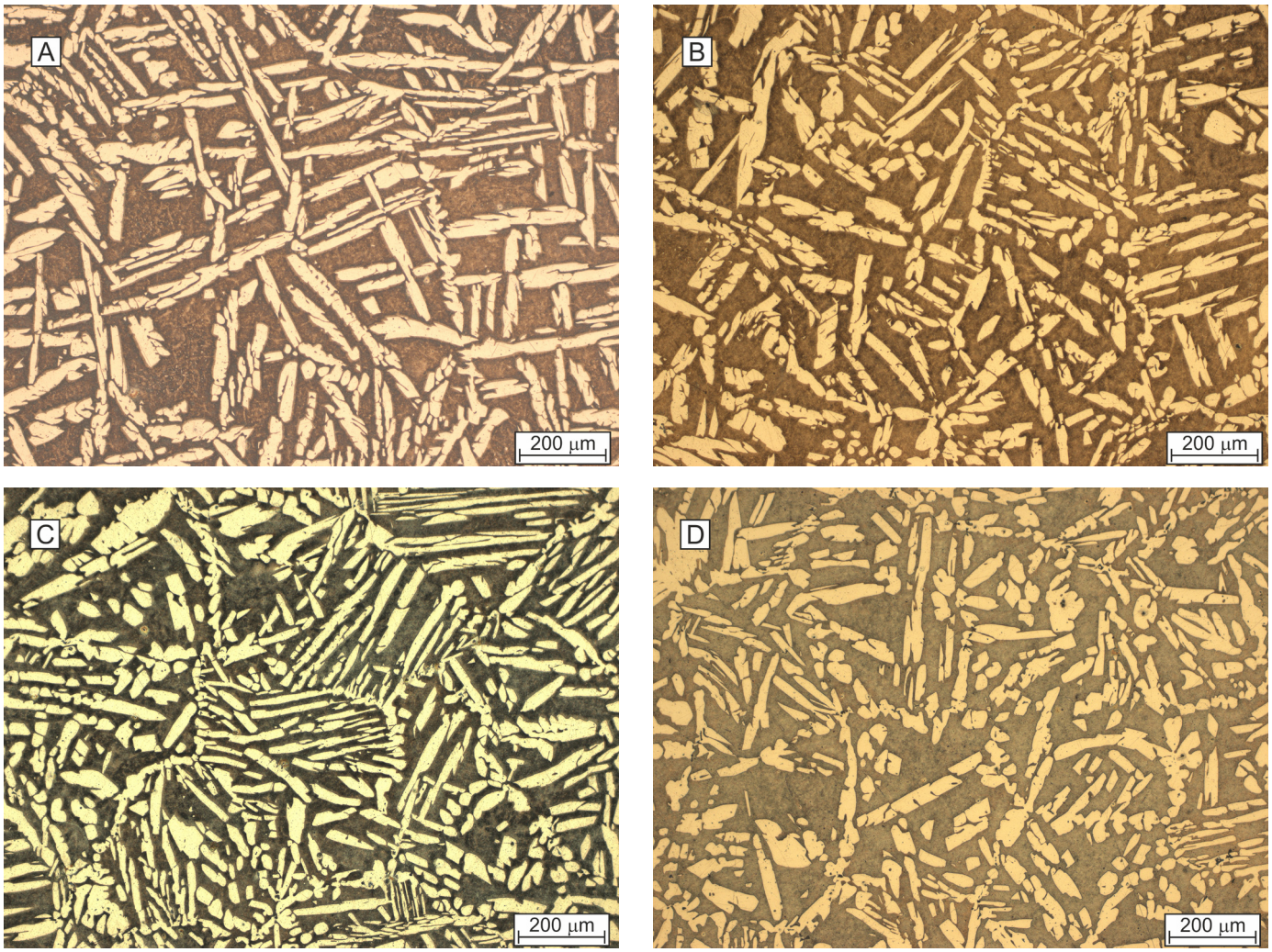

Fig. 1. The microstructure of ternary Mg-Li-Al alloys of compositions: a) Mg-9Li-1.5Al, b) Mg-9Li-1.5Al+0.2TiBor, c) Mg-9Li-1.5Al+0.2Sr and d) Mg-9Li-1.5Al+0.2TiBor+0.2Sr

measurements in points 1-3, Fig. 2), however according to the equilibrium system of Mg-Li, α-(Mg) phase is a solid solution and it must contain approx. 5% of lithium.

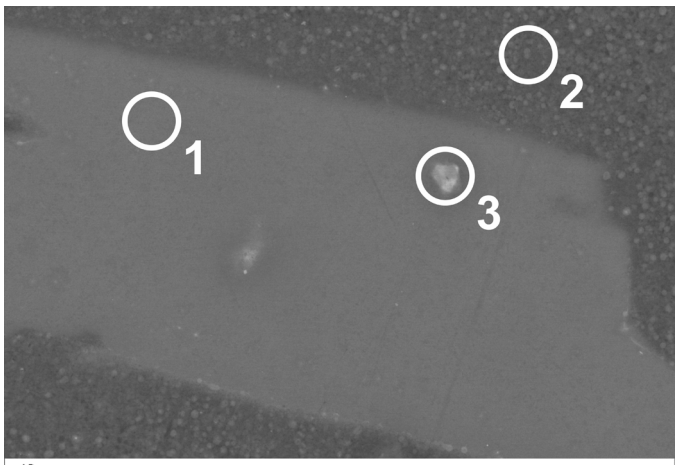

Analysis	Element	wt.%
Point 1	Mg	100
Point 2	Mg	91.1
	Al	2.9
	O	6.0
Point 3	Mg	89.9
	Al	10.1

Fig. 2. SEM image of Mg-9Li-1.5Al alloy modified by 0.2wt.% TiBor master alloy

Fig. 3 shows the SEM morphology and EDS points analyses of the Mg-9Li-1.5Al alloy modified by AlSr10 master alloy. It can be obviously seen that new intermetallic compound with a fishbone-like network is arranged along the grain boundaries. EDS analysis at a location pointed as 4 in the compound area shows that Mg and Sr elements exist in this region. The corresponding mole ratio of Mg to Sr in these compounds is found to be more than 2, so the compound (point 4) could be $Mg_{17}Sr_2$.

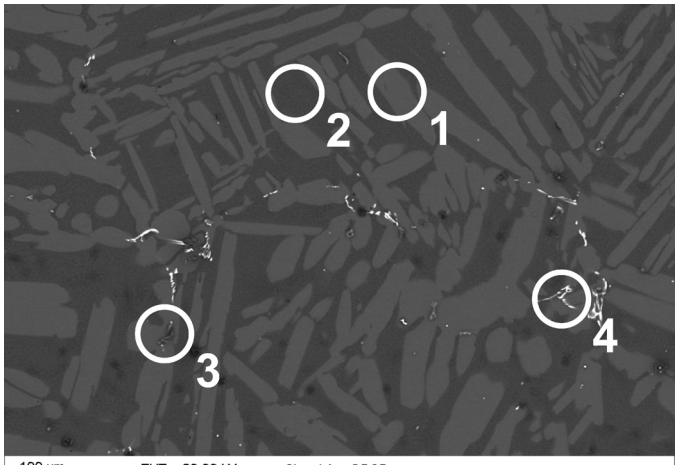

Analysis	Element	wt.%
Point 1	Mg	100
Point 2	Mg	91.6
	Al	2.6
	O	5.8
Point 3	Mg	75.9
	Al	12.3
	O	11.8
Point 4	Mg	73.8
	Sr	26.2

Fig. 3. SEM image and EDS analysis of Mg-9Li-1.5Al alloy modified by 0.2wt.% AlSr10 master alloy

Fig. 4 shows SEM images and EDS analysis of Mg-9Li-1.5Al alloy modified by TiBor and AlSr10 master alloys. From the SEM images and the EDS analyses of Mg, Al, and Sr, it obviously seen that the elements of Mg and Al are uniformly allocated in the entire matrix, the compounds are Mg-rich and Al-rich phases and fishbone-like network compounds are Mg-rich, and Sr-rich phases. Through the ratio of EDS results in Fig. 4 point 3 and 4, it can be determined that the compounds are h(LiAl) phase (Mg come from matrix and Li is not observed in SEM) and fishbone-like network consists of $Mg_{17}Sr_2$ (mole ratio of Mg to Sr is more than 8:1, Al come from the matrix).

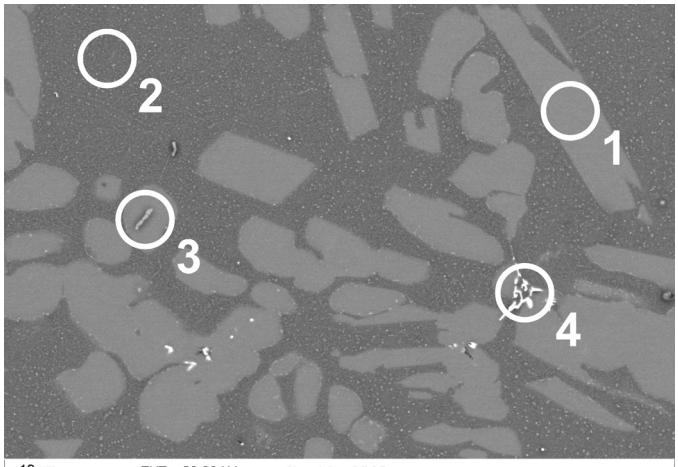

Analysis	Element	wt.%
Point 1	Mg	100
Point 2	Mg	90.9
	Al	3.8
	O	5.3
Point 3	Mg	71.8
	Al	17.3
	O	10.9
Point 4	Mg	85.7
	Sr	11.4
	Al	2.9

Fig. 4. SEM image of Mg-9Li-1.5Al alloy modified by 0.2wt.% TiBor and 0.2wt.% AlSr10 master alloys

In all of investigated the Mg-Li-Al alloys, was found that 3rd primary alloying element such as aluminium is mainly located in β phase (Figs. 2-4 analyses 2) and precipitations marked as 3 in Figs. 3 and 4. Increased content of Mg in analysed points may come from the matrix. Considering Al dissolved in matrix and based on Mg-Li-Al ternary system, it can be concluded that the precipitated compound is h(LiAl). Form and position of recognised compounds in analysed Mg-Li-Al alloys could be directly correlated to the crystallisation process.

The optical micrographs of the samples obtained after thermal analysis are shown in Fig. 5. These micrographs were used to carry out the grain size measurements. The base Mg-9Li-

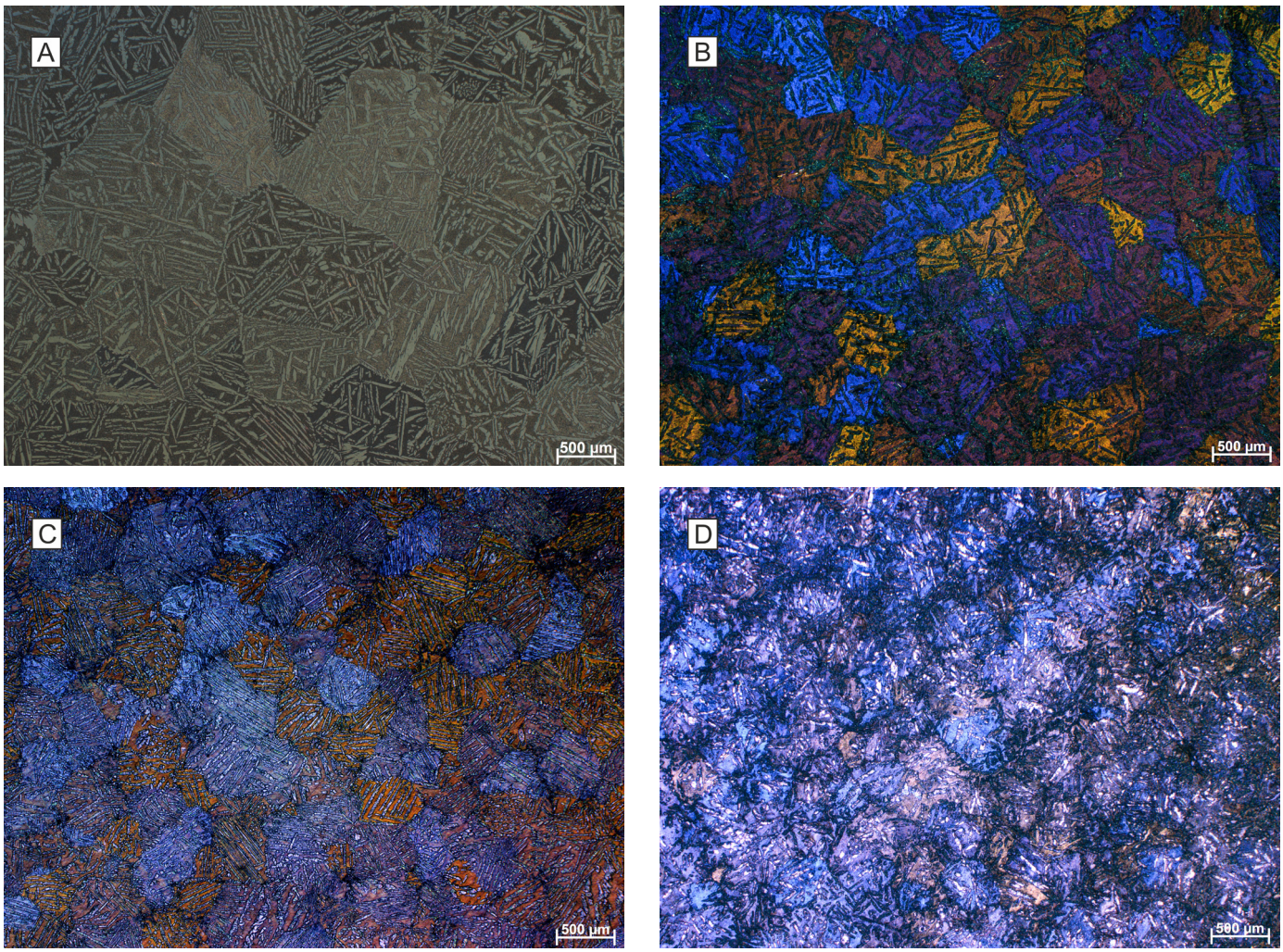

Fig. 5. Microstructure of the grain size for Mg-9Li-1.5Al base alloy at various addition of master alloys: a) Mg-9Li-1.5Al, b) Mg-9Li-1.5Al+0.2TiBor, c) Mg-9Li-1.5Al+0.2Sr, d) Mg-9Li-1.5Al+0.2TiBor+0.2Sr, Nomarsky contrast

1.5Al alloy was observed to have an average grain size of 927.8 ±140 µm. The maximum reduction in grain size was achieved with the addition of 0.2 wt.% TiBor and 0.2 wt.% AlSr10. At this level, there was a 54% reduction in grain size relative to the base alloy, resulting in an average grain size of 431.8±70 µm.

Due to the addition of TiBor master alloy only, the grain size of the Mg-9Li-1.5Al alloy was reduced apparently. When the addition of TiBor was 0.2 wt.%, the mean grain size of base magnesium alloy was reduced to 537±100 µm, that is given a reduction in grain size about 42%.

Although the grain size of Mg-9Li-1.5Al cast alloy containing AlSr10 is, of course, different from that of Mg-9Li-1.5Al cast alloy containing TiBor, their grain refinement efficiencies can still be comparable. It is demonstrated that AlSr10 master alloy had higher grain refinement power than TiBor for Mg-9Li-1.5Al cast alloy.

When the addition of AlSr10 was 0.2 wt.%, the mean grain size of the base alloy was reduced to 480±90 µm, that is given a reduction in grain size about 48%. The average grain size for each addition of master alloy is presented in Figure 6.

The graph indicating the hardness measurements for all of the investigated alloys after thermal analysis is shown in Figure 7.

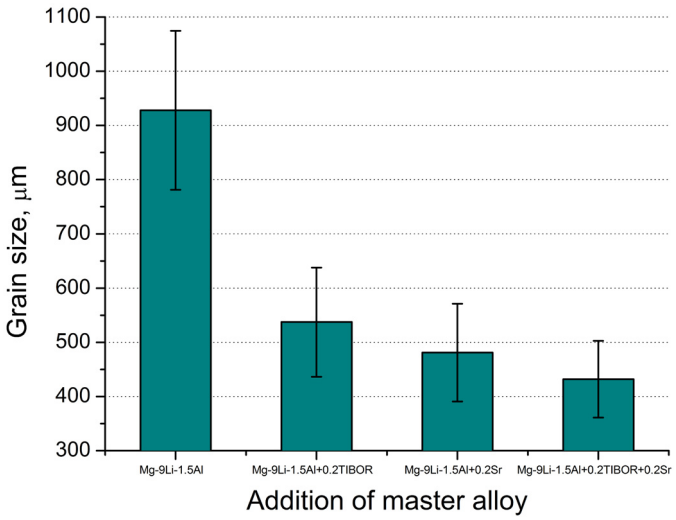

Fig. 6. Grain sizes of Mg-9Li-1.5Al cast alloy with additions of TiBor and AlSr10

The relatively small grain size of Mg-9Li-1.5Al+0.2TiBor+0.2Sr is not obviously reflected in its hardness related with Mg-9Li-1.5Al+0.2TiBor. It can be noted that addition of AlSr10 as grain

refiner slightly increases in hardness. In general, the hardness did not increase with TiBor addition.

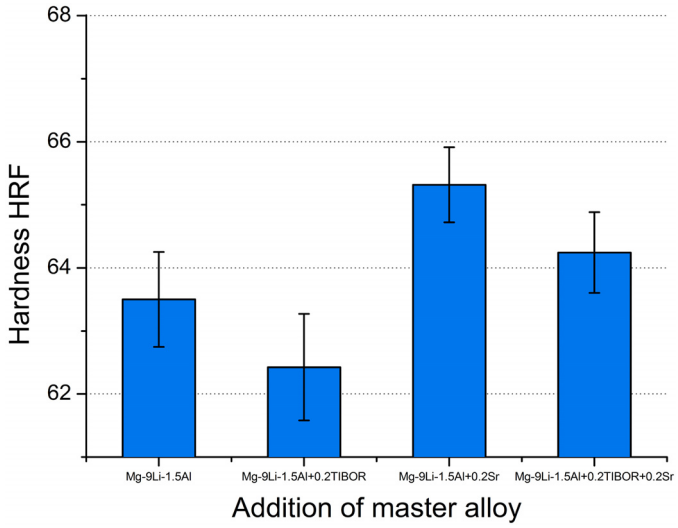

Fig. 7. Hardness of Mg-9Li-1.5Al cast alloy with additions of TiBor and AlSr10

Fig. 8 shows the XRD pattern of the Mg-9Li-1.5Al alloy after thermal analysis untreated and treated by commercial TiBor and AlSr10 master alloys. As shown in Fig. 8, the examined Mg-Li-Al alloys are composed of α-(Mg) and β-(Li). No more peaks correspond to the phases $Mg_{17}Sr_2$ and h(LiAl) were found.

Table 3 and Fig. 9 presents the results from thermal-derivative analysis of Mg-9Li-1.5Al base alloy and modified by

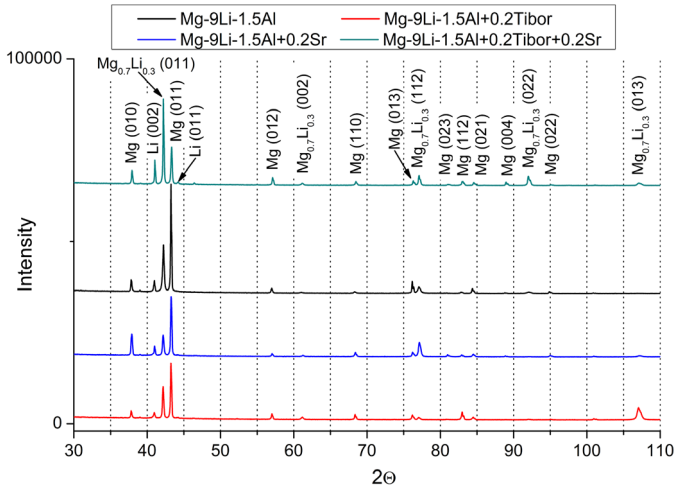

Fig. 8. XRD pattern of investigated Mg-Li-Al alloys

TiBor and Sr. These values represent the temperatures where the respective alloys start and finish solidify.

For Mg-9Li-1.5Al alloy, using the natural cooling rate that was approx. 0.5°C/s, the nucleation temperature of primary β(Li) was recorded at approx. 596.5°C (Fig. 9a). Crystallisation process finished at solidus temperature at around 549.1°C, where remaining liquid changed to solid state. It was found that for analysed Mg-Li-Al alloy, after β(Li) nucleation temperature, intermetallic precipitation of η(LiAl) begin at 552.6°C, 559.1°C and 546.8°C for Mg-9Li-1.5Al+0.2TiBor, Mg-9Li-1.5Al+0.2Sr and Mg-9Li-1.5Al+0.2TiBor+0.2Sr, respectively.

Results from the thermal-derivative analysis (Table 3) presents that the addition of 0.2wt.% TiBor doesn't change the nucleation temperature i.e. 596.3°C, however, decreases the solidus temperature to 536.4°C of investigated magnesium alloys. Modification of Mg-Li-Al alloys by AlSr10 master alloy causes slightly decreases in nucleation temperature to 582.7°C, but strongly reduces a solidus temperature to 535.3°C. The addition of 0.2wt.% TiBor and 0.2wt.% AlSr10 master alloys cause decreases in nucleation temperature and solidus temperature to 579.32°C and 520°C, respectively. It was found that thermal-derivative analysis of modified Mg-9Li-1.5Al alloys reveals an exothermic peak that probably becomes from nucleation of intermetallic compound as η(LiAl) phase [25]; however, more studies must be done. The addition of 0.2wt.% TiBor and 0.2wt.% AlSr10 master alloys decrease a crystallisation range and transition in solid state from 130°C to 105°C. Moreover, an addition of Sr causes a reduction of a time period between the solidus temperature and beginning of α+β reaction in the solid state according to the solvus line in Mg-Li binary system [20,22].

The solidification pathway of investigated Mg-Li-Al based on thermal-derivative analysis, microstructure investigation and SEM and EDS analyses may be proposed as:

1. $L \rightarrow \beta(Li)$
2. $L + \beta(Li) \rightarrow \alpha(Mg) + \eta(LiAl)$
3. $\beta(Li) \rightarrow \alpha(Mg) + \beta(Li)$

At first step in the crystallisation process of Mg-Li-Al alloys, the β-phase (i.e. a solid solution of alloying elements in lithium) starts solidifying, until the liquid composition reaches the point where reaction $L+\beta(Li) \rightarrow \alpha(Mg)+\eta(LiAl)$ taking place (this reaction was registered only for grain modified alloys). In the last stage of the crystallisation process of investigated Mg-Li-Al alloys, transition in solid state, according to the solvus line of Mg-Li binary system occurs causing forming of $\alpha(Mg)+\beta(Li)$ phases.

TABLE 3

Thermal assessments of investigated Mg-Li-Al alloys

Material	1. Nucleation temperature of primary β(Li) °C	2. Nucleation temperature of η(LiAl) °C	3. Solidus Temperature °C	4. Solvus temperature °C	5. End of all transitions °C
Mg-9Li-1.5Al	596.5	-	549.1	505.2	466.2
Mg-9Li-1.5Al+0.2TiBor	596.3	552.6	536.4	501.3	466.6
Mg-9Li-1.5Al+0.2Sr	582.7	559.1	535.3	525.0	473.7
Mg-9Li-1.5Al+0.2TiBor+0.2Sr	579.3	546.8	520	513.2	474.8

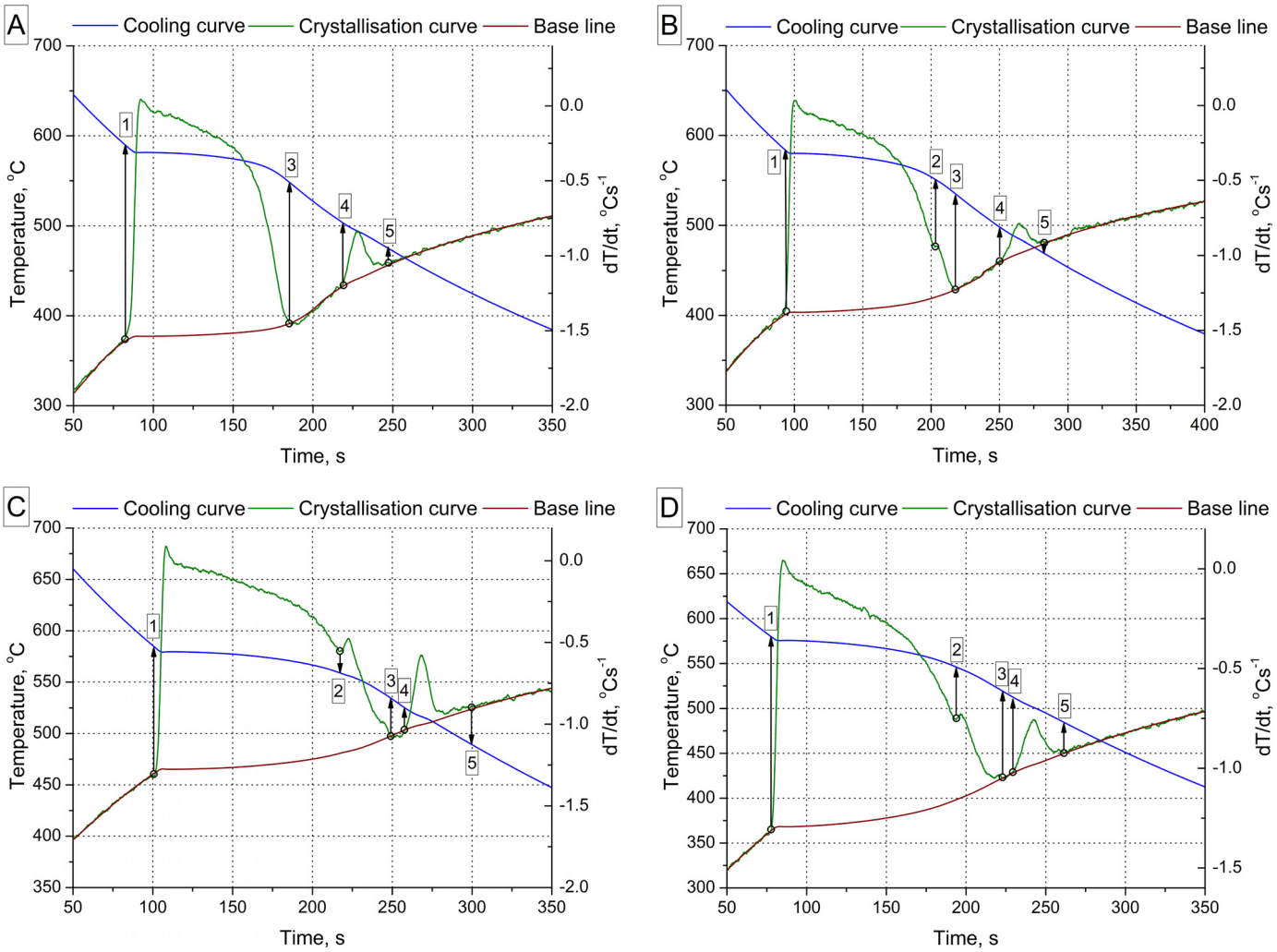

Fig. 9. Representative thermal derivative analysis of investigated Mg-Li-Al alloys: a) Mg-9Li-1.5Al, b) Mg-9Li-1.5Al+0.2TiBor, c) Mg-9Li-1.5Al+0.2Sr and d) Mg-9Li-1.5Al+0.2TiBor+0.2Sr

4. Conclusions

The effect of TiBor and Sr on the nucleation of primary β phase, η(LiAl) intermetallic compound, solidus temperature and solvus temperature has been determined. Moreover, the influence of modifiers on structure and hardness was determined.

Commercially available TiBor and AlSr10 master alloys can be used to refine the grains of cast Mg-9Li-1.5Al alloy. An addition of 0.2wt% the master alloys can reduce the as-cast grain size from 927.8±140 to 431.8±70 µm that is given a reduction in grain size of. approx. 54%, compared to base Mg-9Li-1.5Al.

Based on hardness measurements was found that the addition of AlSr10 refiner slightly increases in hardness. The hardness did not increase with TiBor addition.

Based on thermal-derivative analysis was found that application of 0.2wt.% TiBor and 0.2wt.% Sr master alloys cause decreases in nucleation and solidus temperature. The strongest effect was achieved when two refiners as TiBor and Sr was used simultaneously. Moreover, thermal-derivative analysis can be implemented to registration melting and cooling processes of Mg-Li-Al alloys.

Acknowledgement

This publication was financed by the Ministry of Science and Higher Education of Poland as the statutory financial grant of the Faculty of Mechanical Engineering SUT.

REFERENCES

[1] A. Białobrzeski, J. Pezda, Archives of Foundry Engineering **12** (2), 143-146 (2012).

[2] B. Jiang, Y. Zeng, M. Zhang, H. Yin, Q. Yang, F. Pan, T. Nonferr. Metal. Soc. **23**, 904-908 (2013).

[3] D.H. Stjohn, M.A. Easton, M. Qian, J.A. Taylor, Metall. Mater. Trans. A. **44A**, 2935-2949 (2013).

[4] A. Zieliński, G. Golański, M. Sroka, Mat. Sci. Eng. A-Struct. **682**, 664-672 (2017), DOI: 10.1016/j.msea.2016.11.087.

[5] L.A. Dobrzański, W. Borek, J. Mazurkiewicz, Materialwiss. Werkst. **47** (5-6) SI, 428-435 (2016).

[6] L.A. Dobrzański, M. Czaja, W. Borek, K. Labisz, T. Tanski, Int. J. Mater. Prod. Tec. **51** (3), 264-280 (2015).

[7] A. Zieliński, M. Miczka, B. Boryczko, M. Sroka, Arch. Civ. Mech. Eng. **4**, 813-824 (2016), DOI:10.1016/j.acme.2016.04.010.

[8] A. Zhang, H. Hao, X. Zhang, T. Nonferr. Metal. Soc. **23** (11), 3167-3172, (2013).

[9] R. Wu, Y. Yan, G. Wang, L.E. Murr, W. Han, Z. Zhang, M. Zhang, Int. Mater. Rev. **60** (2), 65-100 (2015).

[10] M. Sun, M.A. Easton, D.H. StJohn, G. Wu, T.B. Abbott, W. Ding, Adv. Eng. Mater. **15** (5), 373-378 (2013).

[11] G. Wei, X. Peng, J. Liu, A. Hadadzadeh, Y. Yang, W. Xie1, Mater. Sci. Technol. **31** (14), 1757-1763 (2015).

[12] T. Mikuszewski, Metalurgija **53**, 588-590 (2014).

[13] T. Mikuszewski, D. Kuc, Inżynieria Materiałowa **35** (3), 258-262 (2014).

[14] I. Bednarczyk, D. Kuc, T. Mikuszewski, Hutnik **83** (8), 321-323 (2016).

[15] R. Cheng, F. Pan, S. Jiang, Ch. Li, B. Jiang, X. Jiang, Prog. Nat. Sci. **23** (1), 7-12 (2013).

[16] V. Kumar, Govind, K. Philippe, R. Shekhar, K. Balani, Procedia Materials Science **5**, 585-591 (2014).

[17] M. Krupinski, B. Krupinska, Z. Rdzawski, K. Labisz, T. Tanski, J. Therm. Anal. Calorim. **120** (3), 1573-1583 (2015).

[18] M. Król, T. Tański, P. Snopiński, B. Tomiczek, J. Therm. Anal. Calorim. 127, 299-308 (2017), DOI 10.1007/s10973-016-5845-4.

[19] R. Schmid-Fetzer, J. Gröbner, Metals **2** (3), 377-398 (2012).

[20] N.C. Goel, J.R. Cahoon, Bulletin of Alloy Phase Diagrams **11** (6), 528-546 (1990), DOI:10.1007/BF02841712.

[21] X. Guanglong, Z. Ligang, L. Libin, D. Yong, Z. Fan, X. Kai, L. Shuhong, T. Mingyue, J. Zhanpeng, Journal of Magnesium and Alloys **4**, 249-264 (2016).

[22] H. Baker, ASM Handbook, Alloy Phase Diagrams, 10th ed., ASM International **3**, 1992.

[23] A. Suzuki, N.D. Saddock, L. Riester, E. Lara-curzio, J.W. Jones, T.M. Pollock, Metall. Mater. Trans. A. **38** (2), 420-427 (2007).

[24] B. Jiang, Y. Zeng, H. Yin, R. Li, F. Pan. Prog. Nat. Sci-Mater. **22** (2), 160-168 (2012).

[25] J. Dutkiewicza, S. Rusz, W. Maziarz, W. Skuza, D. Kuc, O. Hilserb, Acta. Phys. Pol. A. **131** (5), 1303-1307 (2017).